Spectral & Biological Characterization of Zirconyl Complexes of a Pyrazolone-ß-Diketo Hydrazone Ligand

SHIJI FAZIL
Dept. of Chemistry
Mann Aniya College of arts & science, Pangode, Trivandrum.

REENA RAVINDRAN
Dept. of Chemistry,
S.N College, Chempazhanthi, Trivandrum.

Two zirconyl complexes, [ZrO (AAPAAC)$_2$*(NO*$_3$*)*$_2$*] & [ZrO (AAPAAC)*$_2$*Cl*$_2$*], where (AAPAAC= 1,2-dihydro-1-phenyl-2,3-dimethyl-4-[2',4'-pentanedione-3'-hydrazono] pyraol-5-one was synthesized and characterized by physico chemical and spectroscopic methods. The intramolecularly hydrogen bonded hydrazone structure of the ligand, AAPAAC was confirmed by spectral studies (IR, NMR & Mass). The magnetic susceptibility measurements and low conductance data provide evidence for the monomeric and non-electrolytic natures of the complexes respectively. Thermal study of the complexes reveals their stability and anhydrous nature. The ligand shows neutral bidentate behavior in the complexes and the spectral studies confirm an octahedral geometry around the [ZrO]*$^{2+}$*in all the complexes. The ligand and its complexes were screened for their antibacterial activities using disc diffusion methods.*

Keywords: 4-Aminoantipyrine, Acetyl acetone, Hydrazone and Antibacterial.

Introduction

The chemical properties of hydrazone and their complexes are widely explored in recent years, owing to their coordinating ability, pharmacological activity and their use in analytical chemistry as metal extracting agents[1-6].There are various applications of the aroyl hydrazones which depend upon their structural characteristics[7,8]. Due to the electron donating capacity of hydrazones, certain aroyl hydrazones act as inhibitor to prevent the corrosion of copper metal in the presence of nitric acid[9,10]. β -dicarbonyl complexes undergoes diazocoupling at the reactive methylene group and the resultant product exist in intramolecularly hydrogen bonded hydrazone form[11]. Complexes of these types of ligands have been reported and in complexes they may exist as either azo or hydrazo form[11,12]. Here with we are reporting the Zr(IV) complexes of this type of ligand, AAPAAC and here also AAPAAC retains its hydrazone structure when complexed to Zr(IV).

Synthesis

Synthesis of 1,2-dihydro-1-phenyl-2,3-di methyl-4- [2’,4’-pentanedione- 3’ hydrazono] pyrazol-5-one (AAPAAC)

The hydrazone, AAPAAC was prepared by the coupling of acetylacetone with diazotized 4-aminoantipyrine as reported earlier following Japp-Klingemann procedure[11] (Scheme 1) 4-Aminoantipyrine (10.15 g, 50 mmol) was dissolved in 20 ml of ethanol by vigorous stirring and diazotized using $NaNO_2$ (5 g, 72 mmol) and 10 ml of 1:1 HCl by maintaining the temperature below 5 °C. The resulting diazonium salt solution was added slowly with stirring to an ice-cold alkaline solution of acetylacetone (6 ml, 60 mmol) dissolved in 15 ml of 40% NaOH. This mixture was kept in an ice bath for 30 minutes with occasional stirring. Bright shining yellow crystals separated were filtered, washed with petroleum ether and finally with a small amount of water. The product was recrystallised from hot methanol. Melting point is 179 °C. Yield: 80%.

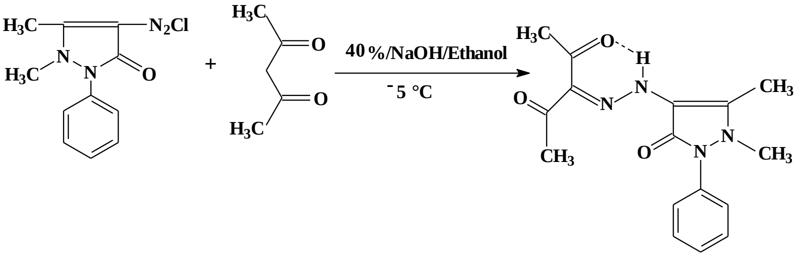

Scheme 1

Synthesis of zirconyl complexes

About 1 mmol of the metal salt [$ZrOCl_2 . 8H_2O$, 0.322 g; $ZrO(NO_3)_2 . H_2O$,0.341 g] was dissolved in methanol. To this a methanolic solution of the ligand (2 mmol, 0.638 g) was added when an instantaneous color change was observed in all the cases. The solution was refluxed for 5-6 h for the completion of the reaction. Solid complexes separated on slow evaporation of the solution were filtered, washed first with benzene and then with ether to remove excess ligand if any and dried over P_4O_{10} under vacuum.

Experimental

Microanalyses of the compounds were done with an Elemental Vario EL III CHN elemental analyzer. Room-temperature FT-IR spectra were recorded as KBr pellets with a JASCO FTIR 4100 Spectrophotometer in the 4000-400cm^{-1} range. The electronic spectra were recorded on a Cary 5000 Version 1.09 UV-VIS-NIR Spectrometer in the range 900-200 nm in methanol solutions. ^1H NMR Spectra of the ligand and complexes were recorded in DMSO-d_6 on a Bruker Avance DRX 500 MHz NMR Spectrometer. The molar conductance of complexes in methanol (10^{-3}M) solutions at room temperature were recorded using a Systronics 303 direct reading conductivity meter. The magnetic susceptibility measurements of the complexes were measured using a Sherwood Scientific magnetic susceptibility balance at room temperature by Gouy method using Hg [Co $(CNS)_4$] as calibrant. The thermal studies were recorded on a Mettler TG-50 thermobalance with 20 °C/min. in nitrogen atmosphere at NIIST, Thiruvananthapuram.

The 3D molecular models of the complex, [ZrO $(AAPAAC)_2Cl_2$],has been constructed by using the Modeling and Analysis Software CHEM BIO 3D Ultra 11.0 [12].

Results and Discussion

The partial elemental analyses data and molar conductivities of the complexes are listed in Table 1. The elemental analysis data of the zirconyl complexes are consistent with their general formulation of the type ML_2X_2, where M = ZrO, L = AAPAAC and X = NO_3^- or Cl^-. The complexes are non-hygroscopic in nature and soluble in acetonitrile, methanol, ethanol, DMF and DMSO.

The low conductance values (in the range 0-18 ohm^{-1} cm^2 mol^{-1}) observed for the 10^{-3} M solutions of complexes in methanol and DMSO suggest non-electrolytic behavior of the complexes.

The magnetic susceptibility of the complexes was found to be negative indicating the complexes are diamagnetic as expected for the $4d^0$ $5s^0$ state of the Zr (IV).

Table – 1

Analytical data and physical data for AAPAAC and its oxometal complexes Composition % Found (Calc) λ_m ($ohm^{-1}cm^2mol^{-1}$)

Compound	Color	Composition % found(calc)			λ_m^a	μ_m^b(B.M)
		Carbon	Hydrogen	Nitrogen		
AAPAAC	yellow	61.26 (61.13)	5.71 (5.77)	17.72 (17.82)	-	-
[ZrO$(AAPAAC)_2Cl_2$]	Blackish brown	47.63 (47.64)	4.59 (4.57)	13.87 (13.89)	6	-
[ZrO$(AAPAAC)_2(NO_3)_2$]	Brown	44.74 (44.76)	4.21 (4.22)	16.29 (16.29)	6.8	-

[a] Molar conductivity, 10^{-3} M methanol at 298 K.
[b] Magnetic susceptibility per metal atom.

Infrared Spectra and Bonding

The IR spectral bands of the ligand, AAPAAC and its zirconyl complexes along with their probable assignments are given in Table 2. Presence of a medium broad band at 3317 cm^{-1} due to the NH stretching and a medium strong band at 1630 cm^{-1} (strongly hydrogen bonded -C=O) in the spectrum of AAPAAC and complexes strongly favours the existence of the intramolecularly hydrogen bonded hydrazone form of the ligand AAPAAC[11]. A strong band at 1720 cm^{-1} indicates the presence of free carbonyl group of the acetylacetone moiety and the presence of this band without much shift in the complexes shows the non-participation of the free –C=O in metal coordination [11,12,13]. This again confirms the existence of the same structure of AAPAAC in metal coordination.

A strong band at 1664 cm^{-1} in the spectrum of AAPAAC can be assigned to the pyrazolone -C=O and the band at 1617 cm^{-1} is attributed to the azomethine group present in the ligand [11, 14,15, 16, 17]. In the spectra of complexes, υC=O (pyrazolone) gets blue shifted by around 30 cm^{-1} showing the participation of this group in complex formation. The, νC=N at 1617 cm^{-1} in AAPAAC also gets shifted to approximately 1580-1590 cm^{-1} indicating the coordination of azomethine nitrogen to the metal atoms [11,18]. From the IR spectra, it is revealed that the ligand, AAPAAC possess a neutral bidentate coordination through the pyrazolone –C=O and the azomethine nitrogen, thus forming a stable six membered ring around the metal atoms under consideration. The zirconyl complexes exhibit one strong band in the region 900 -870 cm^{-1}which can be attributed to the ν(Zr=O) indicating the presence of $(Zr=O)^{2+}$ moiety in these complexes[19]. Monodentate nature of the nitrate in $[ZrO\ (AAPAAC)_2(NO_3)_2]$ is revealed by the presence of strong bands in the region 1376 (ν_4) cm^{-1} and ~1238 (ν_1) cm^{-1} with a medium band at ~1040 cm^{-1}. The separation ~138 cm^{-1} between ν_4 and ν_1 of the nitrate group indicate the presence of terminal monodentate nitrate group [20].

Table - 2
Selected IR bands (cm^{-1}) with tentative assignments of ligand and its metal complexes

Compound	υ(N-H)	υ_{free}(C=O)	$\upsilon_{H\text{-}bonded}$ (C=O)	υ(C=O) pyrazolone	υ (C=N)	υ (N-N)	υ (M-N)
AAPAAC	3310	1720	1630	1664	1602	1140	-
$[ZrO(AAPAAC)_2Cl_2]$	3310	1720	1630	1640	1590	1140	540
$[ZrO(AAPAAC)_2(NO_3)_2]$	3310	1718	1630	1640	1590	1140	553

Electronic spectra

The electronic spectra of most of the zirconyl complexes are difficult to explain due to the formation of high intensity L→M charge transfer bands. The electronic spectra of the zirconyl complexes were recorded in methanol and exhibit bands in the region 240-260 nm (41,667-38,462 cm^{-1}) and 280-300 nm (35,714- 33,333 cm^{-1}) which can be assigned as the π- π^* and n-π^* transitions of ligand, AAPAAC. The broad band around 340 nm (29,412 cm^{-1}) in $[ZrO(AAPAAC)_2Cl_2]$ may be due to the charge transfer bands besides the ligand bands. In $[ZrO\ (AAPAAC)_2(NO_3)_2]$, the broad band around 400 nm (25,000 cm^{-1}) is assigned to the charge transfer bands and the weak broad band observed at 550 nm (18,182 cm^{-1}) is assigned to the O→Zr transition of zirconyl[19,21].

The electronic spectra of zirconyl complexes are presented in Figs.1 &2and the corresponding data in table 3.

Table – 3

Electronic spectral bands of AAPAAC and its oxo metal complexes

Compound	π- π*	n-π*	Charge transfer
AAPAAC	230	290	390
[ZrO(AAPAAC)2Cl2]	255	330	340
[ZrO(AAPAAC)2(NO3)2]	245	325	400

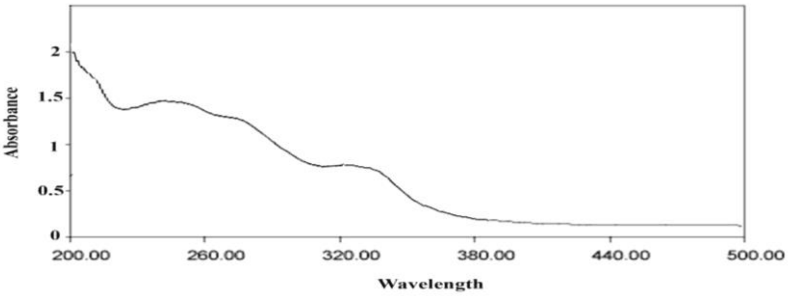

Fig. 1 Electronic spectrum of $[ZrO (AAPAAC)_2Cl_2]$

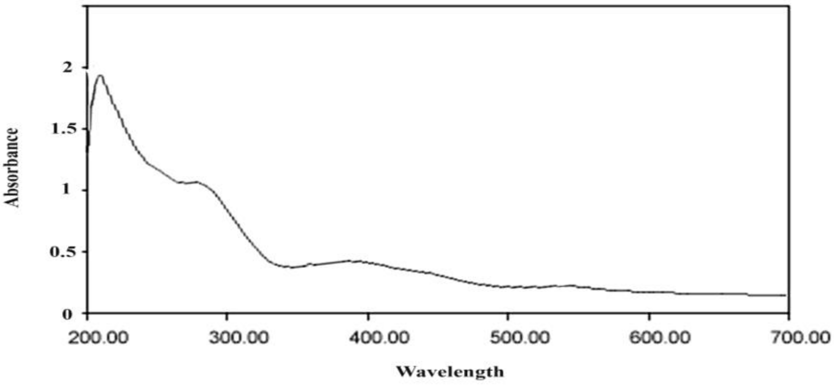

Fig. 2 Electronic spectrum of $[ZrO (AAPAAC)_2(NO_3)_2]$

^{1}H NMR spectra

The ^{1}H NMR spectrum of $[ZrO (AAPAAC)_2Cl_2]$ and AAPAAC in DMSO-d_6 is shown in Table 4. The spectrum of the complex is almost similar to that of the ligand, AAPAAC with minor shifts upon coordination. A singlet at 14.51 ppm in the ligand spectrum is assigned to the proton attached to the nitrogen atom involved in intramolecular hydrogen bonding[11]Existance of this signal at 14.51 ppm in the complex indicates that the same structure of AAPAAC exist in the complex also.

Table – 4

^{1}H NMR spectral assignments of AAPAAC and its oxo metal complexes

Compound	C-CH3	N-CH3	C-CH3 (H-bonded)	C-CH3 free	Aromatic protons	N-H (H-bonded)
AAPAAC	2.25 (3)	3.15 (3)	2.58 (3)	2.40(3)	7.36 – 7.56	14.55
$[ZrO(AAPAAC)_2Cl_2]$	2.26(3)	3.20(3)	2.60(3)	2.40(3)	7.35-7.60	14.51

Thermal Study

Thermal behavior of the complex $[ZrO\ (AAPAAC)_2Cl_2]$ was studied by TGA in nitrogen atmosphere at a heating rate of 10 °C/min. (Fig.3). Thermal decomposition data of the complex is given in Table 5. The thermogram shows that the complex is thermally quite stable. The complex shows gradual loss in weight due to the decomposition of fragments with increasing temperature. The complex is stable up to 200 °C. The complex decomposes in two steps as denoted by the DTG peaks at 250 °C and 500 °C. The initial mass loss of 8.54 % (theoretical 8.79 %) may be due to the elimination of two moles of chlorine molecule from the complex. The second stage of decomposition starts at 443 °C and the final mass loss of 75.91 % (75.94 %) may be due to the corresponding metal oxide [22].

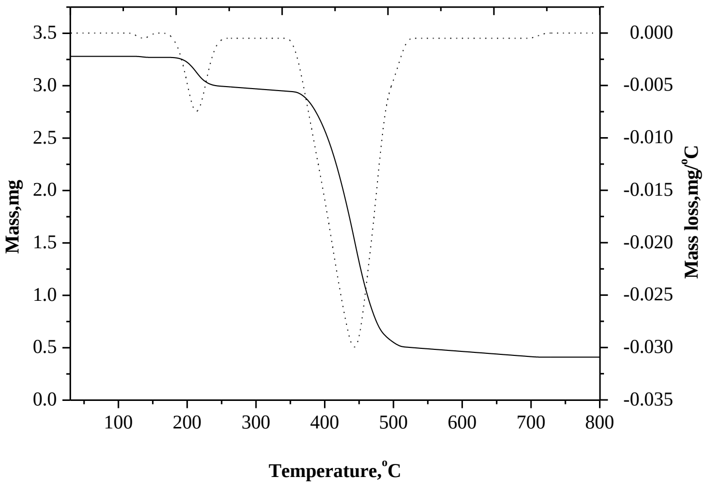

Fig.3 TG/DTG of $[ZrO\ (AAPAAC)_2Cl_2]$

Table – 5

Thermal decomposition of [ZrO $(AAPAAC)_2Cl_2$] and [$UO_2(AAPAAC)_2(NO_3)_2$]

Complex	Stages of Decomposition	Weight loss (%)		Final residue
		TG	Theoretical	
[$ZrO(AAPAAC)_2Cl_2$]	I II	8.79 75.94	8.54 75.91	ZrO_2

The complex is anhydrous, stable up to 230 °C. The complex decompose in two steps as denoted by the DTG peaks at 250 °C and 500 °C. The initial mass loss of 8.54 % (theoretical 8.79 %) may be due to the elimination of two moles of chlorine molecules from the complex. The second stage of decomposition starts at 443 °C and the final mass loss of 75.91 % (75.94 %) may be due to the corresponding metal oxide.

Molecular Modeling

The 3D molecular models of the complex, **[**ZrO $(AAPAAC)_2Cl_2$], has been constructed by using the Modeling and Analysis Software CHEM BIO 3D Ultra 11.0[12]. Fig. 6.14 shows the Chem 3D model of the complex with lowest steric energy. The molecular modeling force fields in use for molecular system can be interpreted in terms of bond stretchings, angle bending, tortional terms and non-bonded interactions (Leach, 2001). The details of the bond lengths and bond angles of the complexes as per 3D structure are shown in Table 6.8. The different bond lengths and bond angles and the various atoms in the compound are numbered in Arabic numerals. Except a few cases, optimal values of both the bond lengths and bond angles are given in the tables along with the actual values. The actual bond lengths and bond angles in the tables are the calculated values as a result of energy optimization in CHEM 3D. The optimal bond lengths /bond angles are the most desirable bond lengths /bond angles established by the builder unit of the CHEM 3D. The missing of some values of standard bond lengths and bond angles may be due to the limitations of the software. In most of the cases, the actual bond lengths and bond angles are close to the optimal values. Thus, the proposed structures of the complexes are acceptable.

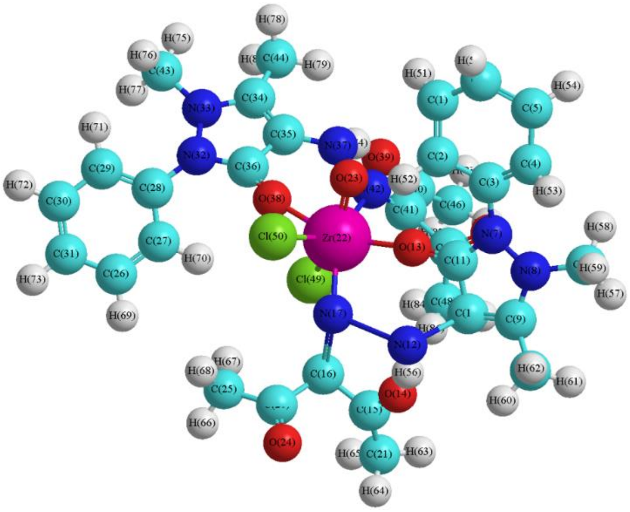

Table - 6

Selected bond lengths and bond angles of [ZrO (AAPAAC)$_2$Cl$_2$]

Atoms	Bond length (Å)	Atoms	Bond angles (°)
Zr(22)-Cl(50)	2.4521	Zr(22)-N(42)-N(37)	119.5790
Zr(22)-Cl(49)	2.4458	Zr(22)-N(42)-C(41)	117.3190
O(38)-Zr(22)	2.0913	Zr(22)-O(38)-C(36)	157.3370
N(42)-Zr(22)	2.1539	Cl(50)-Zr(22)-Cl(49)	116.9420
N(42)-N(37)	1.5664	Cl(50)-Zr(22)-O(38)	73.1616
Zr(22)-O(23)	1.8099	Cl(50)-Zr(22)-N(42)	140.9270
N(17)-Zr(22)	2.1452	Cl(50)-Zr(22)-O(23)	75.7262
O(13)-Zr(22)	2.0964	Cl(50)-Zr(22)-N(17)	72.7699
N(17)-N(12)	2.3695	Cl(50)-Zr(22)-O(13)	111.0450
		Cl(49)-Zr(22)-O(38)	72.7462
		Cl(49)-Zr(22)-N(42)	77.9544
		Cl(49)-Zr(22)-O(23)	146.4330
		Cl(49)-Zr(22)-N(17)	84.0703
		Cl(49)-Zr(22)-O(13)	120.5540
		O(38)-Zr(22)-N(42)	78.2963
		O(38)-Zr(22)-O(23)	82.8556
		O(38)-Zr(22)-N(17)	123.0830
		O(38)-Zr(22)-O(13)	157.2480
		N(42)-Zr(22)-O(23)	74.7293
		N(42)-Zr(22)-N(17)	146.2830
		N(42)-Zr(22)-O(13)	86.3716
		O(23)-Zr(22)-N(17)	129.1620
		O(23)-Zr(22)-O(13)	76.9008
		N(17)-Zr(22)-O(13)	78.5145
		Zr(22)-N(17)-N(12)	117.3540
		Zr(22)-N(17)-C(16)	113.0460
		Zr(22)-O(13)-C(11)	170.6150

Fig. 4 Optimized geometry of [ZrO (AAPAAC)$_2$Cl$_2$]

Antibacterial Studies

The ligand, AAPAAC and its two zirconyl complexes have been screened for antibacterial activity against Gram-negative *Eschericia coli* and Gram-positive *Bacillus cereus* using the disc diffusion method[23,24]. As a reference standard, *Streptomycin* was used. The data obtained showed that the complexes were weakly active against *E. coli and B. cereus.* The ligand had the largest zone of inhibition, which was against *Bacillus cereus* (inhibition zone diameter of 9 mm; 0.1 mg/ disc).

Conclusion

Two zirconyl complexes of the pyrazolinyl hydrazone ligand, AAPAAC has been synthesized and characterized on the basis of their various physico chemical studies. The electrical conductance studies show that the two complexes are non-electrolytic in nature. Magnetic measurement studies reveal the diamagnetic nature of the complexes. Electronic spectra of the complexes are also consistent with the observed magnetic measurement. The electronic spectra show the intralingual and charge transfer transitions. Infrared spectra show the coordination of metal ions through the pyrazolone oxygen and through the azomethine nitrogen. In all the complexes the ligand act as a neutral bidentate and there is a six coordinated structure around $(ZrO)^{2+}$. The ^1H NMR study of the zirconyl complexes reveal the existence of the intramolecularly hydrogen bonded hydrazone form of AAPAAC in the complex also. Thermal study of the complex, $[ZrO(AAPAAC)_2(Cl)_2]$ indicates the thermal stability and the anhydrous nature of the complex studied. The following tentative structures satisfactorily explain the experimental observations.

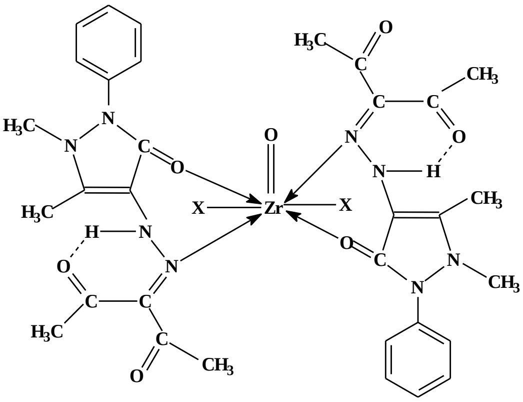

X = Cl$^-$ or NO_3^-

Fig. 5 Proposed structure of $[ZrO(AAPAAC)X_2]$

Reference

Gup R, Kirkan B (2005) Spectrochim Acta 62:1188-1195.

Song QB, Lu ZL, Wu XL, Ma YX (1994) Trans Met Chem 19 :503-505.

Busto.s C, Sanchez. C, Martinez R, Ugarte R, Schott E, Carey D. M, Garland M. T, Espiniza L (2007) Dyes and Pigments 74:615-621.

Rollas. S, Gulerman. N, Erdeniz. H (2002) II Farmaco 57:171-174.

Cacic. M, Trkovnik. M, Cacic. F, Has-Schon E (2006) Molecules 11:134-147.

Bedia KK, Elcin O, Seda U, Fatman K, Nathaly S, Sevim R, Dimoglo A (2006) Eur J Med Chem 41:1253-1261.

Raman N, Sakthivel A, Rajasekaran K (2007) Microbiology 35:150-153.

Kuznetsov M. L, Demntev A. I, Zhornik V. V (2001) J Mol Struct (Theochem) 571:45-57
Dontsova E. V, Lukov U. V, Kogan UA, Popov LD (2003) Russian J Coord Chem 29:639-642.

Bishop E (1972) Indicators International Series of monographs in analytical chemistry, Pergamon Press, Oxford.

Ravindran R (2004) Ind J Chem 43:1245-1248.

Chem Bio Office, ‘Ultra Molecular and Analysis’ , Cambridge, Available from www.cambridgesoft.com.

Kala U. L, Suma S, Kurup M. R. P, Krishnan S, John RP (2007) Polyhedron 26:1427-1435.

Raman N, Raja JD (2007) Ind J Chem 46: 1611- 1614.

Kuriakose M, Kurup MRP. Suresh E (2007) Spectrochim Acta 66: 353-358.

Krishnankutty K, Reena VT (1995) Synth React in Org Met Org Chem 25:243-256.

Krishnankutty K, Venugopalan P (1998) Synth React in Org Met Org Chem 28:1313-1325.

Siji V. L, Sudarsanakumar M. R, Suma S, Kurup MRP (2010) Spectrochim Acta 76:22-28

Mohapatra, R. K.; Dash, D. C. *J. Kor. Chem. Soc.*, **54**, 2010, 395-401.

Nakamoto K (1997) Infrared and Raman Spectra of Inorganic and Coordination Compounds, Part B, 5th Ed, Wiley, New York.

Sathyanarayana DN (2004) Vibrational Spectroscopy, New Age International, New Delhi.

Raman. N, Kulandaisamy. A, Thangaraja. C (2004) Trans Met Chem 29 :129-135.

Chandra S, Sharma AK, Spectrochim Acta (2009) 72:851-857.

Collins C. H, Lyne P. M (1970) Microbiological Methods, University Park Press, Baltimore.